

**Synthesis of chitosan polysaccharide nanoparticles for skin grape extract stabilization****Síntese de nanopartículas a partir do polissacarídeo quitosana para estabilização de extrato da casca de uva**

DOI:10.34117/bjdv6n4-094

Recebimento dos originais: 14/03/2020

Aceitação para publicação: 06/04/2020

**Cristina Barbosa da Silva,**

Formação: Chemistry graduation

Instituição: Brazilian Agricultural Research Corporation - Embrapa Semiárid

Endereço: Rodovia BR-428, Km 152, Zona Rural, CP 23, 56302-970, Petrolina - PE, Brazil.

e-mail: cristinny.live@hotmail.com

**Dirliane Santos Duarte**

Formação: Chemistry graduation

Instituição: Universidade Federal do Vale do São Francisco - CPG Ciência dos Materiais

Endereço: Av. Antonio Carlos Magalhães, 510, CEP: 48902-300, Juazeiro - BA, Brazil

e-mail: dirlianeduarte@gmail.com

**Ana Valéria Vieira de Souza,**

Formação: PhD in Horticulture

Instituição: Brazilian Agricultural Research Corporation - Embrapa Semiárid

Endereço: Rodovia BR-428, Km 152, Zona Rural, CP 23, 56302-970, Petrolina - PE, Brazil.

e-mail: ana.souza@embrapa.br

**Odilio Benedito Garrido Assis**

Formação: PhD in Materials Science and Engineering

Instituição: Brazilian Agricultural Research Corporation - Embrapa Instrumentation

Endereço: Rua XV de Novembro, 1.452, Centro, CP 741, 13560-970, São Carlos - SP, Brazil.

e-mail: odilio.assis@embrapa.br

**Douglas de Britto**

Formação: PhD in Physical Chemistry

Brazilian Agricultural Research Corporation - Embrapa Semiárid

Endereço: Rodovia BR-428, Km 152, Zona Rural, CP 23, 56302-970, Petrolina, PE, Brazil.

e-mail: douglas.britto@embrapa.br

**ABSTRACT**

Nanoparticles obtained by chitosan and tripolyphosphate has been largely studied due to its entrapment characteristics. However, several parameters can influence the synthesis and encapsulation processes. In this way, this work proposed to study the nanoparticle formation with chitosan and tripolyphosphate in function of the acid concentration (1.0; 0.5 and 0.1%) and the kind of the acid (hydrochloric and acetic). Conductometric and Potentiometric techniques showed that the reactional system was very dependent on the pH variation. The best condition, both for HCl and acetic acid, was achieved for systems with lower pH variation. For such systems, Dynamic Light Scattering technique showed formation of nanoparticle with the lowest size ( $135\pm 7$  nm) and higher

stability (zeta potential near 30 mV). Also, by Scanning Electronic Microscopy, such systems exhibited good morphological aspect, with nanoparticles having spherical shape and lower level of agglomeration. The cryoprotection with sucrose solution before freeze-drying was fundamental to get samples with the improved re-suspension ability and preserved nanoparticle character. By UV-visible spectrophotometry, both HCl and acetic acid-based systems resulted in nanoparticles with good polyphenols encapsulation efficiency (~70%). The release profile was pH-dependent. In this way, the chitosan and tripolyphosphate ionic gelification need an accurate pH control both in the synthesis and in the encapsulation-release processes.

**Keywords:** Hydrogel; Polyelectrolyte; Ionic crosslinking; Polyphenols; Encapsulation.

## RESUMO

Nanopartículas obtidas a partir de quitosana e tripolifosfato têm sido amplamente estudadas devido às suas características de encapsulamento. No entanto, vários parâmetros podem influenciar nesse processo. Dessa forma, este trabalho propôs estudar a formação de nanopartículas com quitosana e tripolifosfato em função da concentração de ácido (1,0; 0,5 e 0,1%) e do tipo de ácido (clorídrico e acético). As técnicas condutométricas e potenciométricas mostraram que o sistema reacional foi dependente da variação do pH. A melhor condição, tanto para HCl quanto para ácido acético, foi alcançada para sistemas com menor variação de pH. Para esses sistemas, a técnica de Espalhamento Dinâmico de Luz mostrou formação de nanopartículas com o menor tamanho ( $135 \pm 7$  nm) e maior estabilidade (potencial zeta próximo a 30 mV). Além disso, por Microscopia Eletrônica de Varredura, esses sistemas exibiram aspecto morfológico regular, com nanopartículas com formato esférico e menor nível de aglomeração. A crioproteção com solução de sacarose antes da liofilização foi fundamental para obter amostras com a capacidade de ressuspensão aprimorada e o caráter de nanopartícula preservada. Por espectrofotometria visível no UV, os sistemas baseados em HCl e ácido acético resultaram em nanopartículas com boa eficiência de encapsulamento de polifenóis (~70%). O perfil de liberação foi dependente do pH. Dessa forma, a gelificação iônica de quitosana e tripolifosfato precisa de um controle preciso do pH, tanto na síntese quanto nos processos de liberação do encapsulamento.

**Palavras-chave:** Hidrogel; Polieletrólito; Reticulação iônica; Polifenóis; Encapsulamento.

## 1 INTRODUCTION

The main challenging in working with nanoparticles (NP) synthesis from polyelectrolyte polysaccharides is its dependency on factors related to shape and structure. The polysaccharide concentration, the ratio of polymer-crosslinking agent and the presence of a third component (salt, encapsulated substance, etc.) can be assumed as the main interfering factors in NP synthesis. Particularly for chitosan, several studies have been conducted in an attempt to a better attribution of such parameters. In one of them, it was evaluated the influence of the chitosan molecular weight, the ratio of crosslinking agent tripolyphosphate (TPP) and the pH on the final size and zeta potential of synthesized NP [1]. Concerning the NP sizes, it increases steadily with chitosan concentration, equally for low, medium or high molecular weight chitosan. Small-sized NP could be achieved by reacting a low concentration of low or medium molecular weight chitosan. Besides, the same authors reported that the ratio of chitosan to TPP also influence the NP structure significantly, increasing in size as the proportion of TPP is increased. In this way, chitosan to TPP mass ratio

should be around 3:1 or 3:2 [1]. Recent optimization study based on factorial design has confirmed such chitosan to TPP mass ratios [2,3]. The 3-D surface responses have also confirmed the influence of the increasing of chitosan concentration and its rate to TPP on the NP size.

However, such chitosan-TPP system requires further optimization if a third species is included, for example, the addition of a compound or molecule to be encapsulated [2,4]. In this scenario, it is clear that the characteristics of each substance will interfere on the NP architecture as well as on its encapsulation efficiency [5]. The understanding of such polyelectrolyte-TPP-encapsulated substance structure is fundamental for the practical application of the chitosan NP in biological systems [6-8]. Multicomponent substances such as essential oils and polyphenols extracts increase even more the complexity of the system. However, due to its potential application, for example, as polymeric films [9,10], it must be studied.

Particularly for the polyphenols obtained from grape extract, they are widely studied due to its broad range of biological effects as antioxidants, antimicrobials, and modulators of various enzyme systems. Beneficial effects for human health have been demonstrated in experimental studies for cardiovascular diseases, cancer, diabetes, neurodegenerative diseases and many others [11]. Based on this, polyphenol has been added to polymers in forms of nanoparticle and nanocomposite [12,13]. In the Agricultural sector, polyphenols can be useful as an active antifungal ingredient in edible coatings to extend the shelflife of perishable fruits and vegetables [14,15].

In the face of the complexity of this multivariable system, it is necessary to understand the basic principle that leads the NP formation. Particularly for chitosan, the ionic crosslinking with specific polyanions is a widely used technique [16]. Chitosan can form gel spontaneously on contact with multivalent polyanions due to the network formation of inter- and intramolecular cross-linking [4]. Among the investigated polyanions, the TPP has been distinguished due to its non-toxic nature, quick gelling ability and easy interaction under mild conditions, configuring as the most promising system for processing NP carriers for macromolecules delivering [1,16].

Based on this, aiming a better control of the synthesis and encapsulation, the present study explores the influence of the acid solvent on the NP formation. It is discussed if different anions from acids, e.g.,  $\text{Cl}^-$  or  $\text{CH}_3\text{COO}^-$ , in different concentration, has some influence upon the NP architecture. Also, the encapsulation efficiency of the improved NP with grape skin extract is evaluated as well as its release property, focusing the potential application in agricultural, food and biomedical areas.

## 2 MATERIALS AND METHODS

### 2.1 MATERIALS

Sodium tripolyphosphate (TPP) and medium molecular weight chitosan (Chi), 80% deacetylated, were purchased from Aldrich Chemical Company Inc. (USA) and used as supplied. Hydrochloric acid (37%, p.a. – ACS reagent) and glacial acetic acid were acquired from Alphatec (Brazil) and Vetec (Brazil) respectively. The byproduct from winery activity (*Vitis Vinifera*, ‘Egiodolla’ variety) was supplied by ViniBrasil enterprise, located in Petrolina, PE, Brazil.

### 2.2 DETERMINATION OF FREE ACID IN CHITOSAN SOLUTION BY CONDUCTOMETRIC TITRATION

Initially, the unbounded amount of acid used to prepare chitosan solution was determined by conductometric titration. For this, chitosan solutions of  $3.0 \text{ mg cm}^{-3}$  were prepared in three acid concentrations: 1.0; 0.5 and 0.1% (v/v) by using hydrochloric and acetic (HAc) acids. The solutions were titrated with 0.5 M aqueous sodium hydroxide solution and the electrical conductivity monitored with a digital conductometer (Digimed DM-3P, Brazil).

### 2.3 DETERMINATION OF THE PH VARIATION AND NP YIELDING

The NP were synthesized according to the sequence previously described [5]. Two aqueous TPP solutions ( $50.0 \text{ cm}^3$ ) at  $0.6 \text{ mg cm}^{-3}$  or  $1.2 \text{ mg cm}^{-3}$  were prepared and added drop-wise to  $50.0 \text{ cm}^3$  of chitosan solutions ( $3.0 \text{ mg cm}^{-3}$ ) at the different acid concentrations (as formerly described). The initial and final pH was recorded (pH-meter Digimed DM-3P, Brazil). For the determination of yielding (recovered mass), after the pH measuring the sample was centrifuged at 20,000 RPM (~43,000 RCF) in a centrifuge (Beckman Coulter, model Avanti J26-XP, California, USA) for 20 minutes and  $5^\circ\text{C}$ . The precipitated NP was freeze-dried before mass determination.

### 2.4 CHARACTERIZATION OF THE NP IN THE FUNCTION OF THE ACID KIND AND CONCENTRATION

The size, zeta potential and morphology were considered the most significant characteristics to be evaluated in the chitosan-TPP NP processing. For this, the NP synthesis was performed in two different chitosan solvent acids (HCl and  $\text{CH}_3\text{COOH}$ ) at concentrations of 1.0; 0.5 and 0.1%, and the resulting particles analysed by Dynamic Light Scattering (DLS, Malvern Instruments Ltd., model ZS Zen 3600, Worcestershire, United Kingdom). This allowed determining both size and zeta potential.

The morphology of the chitosan NP was evaluated by Scanning Electronic Microscopy (SEM). After the synthesis, the suspension was centrifuged (as described above), the supernatant discarded and the NP freeze-dried. The dry powder was re-suspended in water and deposited onto a glass sheet for gold deposition and SEM observation (Tescan, model Vega 3, Kohoutovice, Czech Republic). In addition, some NP precipitated was submitted to cryoprotection pre-treatment with sucrose solution at 5.0% (w/v) in water and freeze-dried. After the drying, the powder was washed three times with deionized water to remove the excess of sucrose and re-suspended in water. Aliquots were deposited onto a glass sheet for pre-evaluation by Optical Microscopy (OM) with a microscopy Coleman, N107T, Brazil. Some samples submitted to cryoprotection pre-treatment were also observed by SEM as described above.

## 2.5 EXTRACTION AND ENCAPSULATION OF POLYPHENOLS

The methodology for extraction of polyphenols was based in a hydro-alcoholic extraction. For this, at first, the seeds were separated from the wine byproduct and 200 g of grape skin was extracted with water-ethanol, as described in the literature [17]. After the filtration, rotaevaporation and lyophilization, a dry material was obtained and stored in the dark at -20 °C until utilization. The polyphenol extract was then encapsulated in the chitosan NP, as described in item 2.3, with the previous addition of 80.0 mg dry extract to the TPP solution (50.0 cm<sup>3</sup> at 1.0 mg cm<sup>-3</sup>). The 50.0 cm<sup>3</sup> of chitosan solution (3.0 mg cm<sup>-3</sup>) was prepared both in HAc and in HCl at 0.5% (v/v).

For determination of Encapsulation Efficiency (EE), it was used an UV-visible spectrophotometer from Thermo Fisher Scientific®, model Multiskan GO, Waltham, MA USA. First, the NP suspension was centrifuged at 20,000 RPM for 20 minutes at 8 °C and the supernatant quantified for the phenolic compound. For this, calibrations curves were set with appropriated concentrations of freeze-dried skin grape extract in ethanol-water solution (1:1). The maximum absorbance in the UV-Visible spectrum (200-400 nm range) was 278 nm. The resultant calibration curve fit was  $y = -0.1878 + 8.7375x$  ( $R^2 = 0.9738$ ).

NP with encapsulated extract was also evaluated for the release profile. For this, 10.0 g of centrifuged hydrogel was suspended in 60% ethanol-phosphate buffer solution (40.0 cm<sup>3</sup>) under orbital agitation at 120 RMP and 25 °C. At pre-determinate time intervals, aliquots of the solution were analyzed by UV-Visible spectroscopy, as described above. The freeze-dried NP with encapsulated extract was also evaluated for the release profile. For this, 100.0 mg of freeze-dried NP was dispersed in 60% ethanol-phosphate buffer solution (20.0 cm<sup>3</sup>) and proceeded as above. For release experiment in different pH, this was adjusted with HCl or NaOH solution at 1N. The experiment was done in duplicate.

### 3 RESULTS AND DISCUSSION

For the solubilization of chitosan, it is necessary to have a minimum amount of  $H^+$  in the solvent in order to protonate the chitosan amino moieties. This minimum  $H^+$  amount is not easy to be determined due to the polyelectrolyte nature of the chitosan. An exact determination requires the accurate measurement of the degree of deacetylation, transport coefficient and degree of dissociation [18]. However, considering that the most reported acid concentration for solubilizing chitosan is 1.0% (or even 2.0% v/v), it is quite evident that there is a great excess of  $H^+$  in the solution. The titration curve of Chi-HCl at 0.5% confirm such fact in which the graph shows three different slopes (Figure 1a). The first branch of the graph corresponds to the neutralization of  $H^+$  in excess due to high molar conductivity of ions  $H^+$  and  $Cl^-$  when compared to the conductivity of  $Chi-NH_3^+$ . The second branch is generated by the neutralization of  $Chi-NH_3^+$ . Finally, the third slope is related to the increase of the conductivity due to the NaOH excess [18]. On the other hand, for the titration of Chi-HCl at 0.1%, it is not possible to identify the first branch, related to the excess of  $H^+$ . It is important to highlight that despite this low  $H^+$  concentration, the chitosan mass was fully soluble. In this case, the concentration of  $H^+$  is assumed to be near the minimum necessary to solubilize the chitosan. Theoretically, by considering the HCl concentration (37%) and its density ( $1.19 \text{ g cm}^{-3}$ ), when in solutions at 0.1 and 0.5% (v/v) the concentration of  $H^+$  must be 0.0121 and 0.0603 M, respectively. In fact, these lowest concentrated acid solutions are very close to the stoichiometry of the glucosamine in the chitosan structure, that is 0.0140 ~ 0.0158 M, considering  $50 \text{ cm}^3$  at the concentration of  $3.0 \text{ mg cm}^{-3}$  and degree of deacetylation ranging from 75 to 85%. Also, considering the  $1.29 \text{ cm}^3$  volume of NaOH at 0.5 M used to neutralize exclusively the protonated  $Chi-NH_3^+$ , it is found an equivalent of  $6.5 \cdot 10^{-4} \text{ mol}$ . Such value is very close to  $7.45 \cdot 10^{-4} \text{ mol}$  of glucosamine calculated for  $50 \text{ cm}^3$  at  $3.0 \text{ mg cm}^{-3}$  and degree of deacetylation approximately 80%.



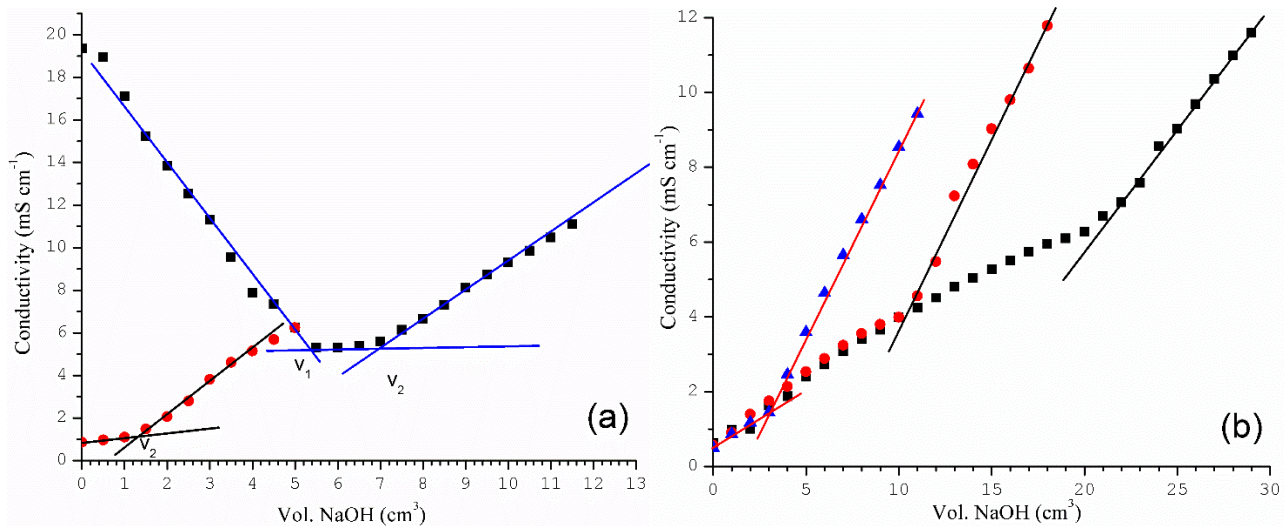


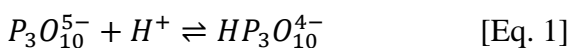
**Figure 1.** Conductimetric titration curves for chitosan acid aqueous solution (3.0 mg cm<sup>-3</sup>) with NaOH 0.5 M for **a)** hydrochloric acid at 0.5% (■) and 0.1% (●) (v/v) and **b)** acetic acid at 1.0 (■); 0.5 (●) and 0.1% (▲) (v/v).

The titration of Chi-HAc had a different aspect, resulting in a two-branch graph (Figure 1b). This occurs in reason of differences in strength, conductivity and degree of dissociation of CH<sub>3</sub>COOH when compared to HCl system. In this way, it was not possible to identify any change of inclination in the titration curve, preventing the determination of the H<sup>+</sup> in excess. However, considering that the chitosan was fully dissolved at the lowest 0.1% acetic acid solution and its titration curve was similar to that at high acid concentration, it is possible to affirm that this lowest acid concentration is sufficient to solubilize the chitosan without an excess of H<sup>+</sup>. Moreover, considering the density of glacial acetic acid (1.049 g cm<sup>-3</sup>), the 0.1% acetic solution results in a 0.0175 M that is close to 0.0140 ~ 0.0158 M for glucosamine in the solution.

In the face of these numerical relations, it is clear that the concentration of 1.0% acetic acid generally used to solubilize chitosan and prepare nanoparticles has a great excess of H<sup>+</sup>, which may influence the particles architecture [1] as well as its encapsulation efficiency.

#### 4 INFLUENCE OF THE ACID ON THE PH VARIATION AND YIELDING

TPP is a moderated conjugated base. The aqueous TPP solution at 1.2 mg cm<sup>-3</sup> and 0.6 mg cm<sup>-3</sup> resulted in respective pH 9.58 and 9.69. Pentabasictriphosphoric acid, H<sub>5</sub>P<sub>3</sub>O<sub>10</sub>, has pK<sub>a</sub> of 1.0, 2.2, 2.3, 3.7 and 8.5 [19]. Consequently, it is found partially undissociated at acid chitosan solution (Eq. 1), which will influence the pH equilibrium during the NP synthesis.



In fact, according to Table 1, the pH of the solution showed significant change after the synthesis. For Chi-HAc at fixed chitosan ( $3.0 \text{ mg cm}^{-3}$ ) and TPP ( $1.2 \text{ mg cm}^{-3}$ ) concentrations, by varying only the acid concentration, the  $\Delta\text{pH}$  increased inversely proportional with respect to the acid concentration. This means that some fraction of TPP is, in fact, reacting with the  $\text{H}^+$  from  $\text{CH}_3\text{COOH}$ . Therefore, as more diluted the acetic solution, less ionic species will be available to react, then the pH variation will be large. However, this last condition ( $\text{CH}_3\text{COOH} = 0.1\%$  and  $\text{TPP} = 1.2 \text{ mg cm}^{-3}$ ) resulted in precipitation of NP, indicating the formation of larger particles. By fixing the  $\text{CH}_3\text{COOH}$  concentration at  $0.1\%$  and decreasing the TPP concentration to  $0.6 \text{ mg cm}^{-3}$ , the resulted  $\Delta\text{pH}$  was not much different from that measured at  $\text{TPP} = 1.2 \text{ mg cm}^{-3}$ . However, this resulted in profound changes in the NP characteristics, as will be discussed in the next item. A similar trend was observed for Chi-HCl solution, which  $\Delta\text{pH}$  also has changed greatly when fixing TPP at  $0.6 \text{ mg cm}^{-3}$  and varying the acid concentration. In accordance, by combining more diluted acid solution ( $0.1\%$ ) with a more concentrated TPP solution ( $1.2 \text{ mg cm}^{-3}$ ), the changes in the  $\Delta\text{pH}$  was reduced, but the formed NP also have precipitated.

**Table 1.** pH variation and yielding in the synthesis of NP from chitosan solution ( $3.0 \text{ mg cm}^{-3}$ ) in HCl and acetic acids solutions at different concentrations.

Samples	TPP conc. ( $\text{mg cm}^{-3}$ )	pH <sub>i</sub>	pH <sub>f</sub>	$\Delta\text{pH}$	Yielding (mg)
NP HAc 1.0%	1.2	2.71	3.75	1.04	97.4
NP HAc 0.5%	1.2	2.93	4.14	1.21	45.6
NP HAc 0.1%	1.2	3.30	5.58	2.28	31.4
	0.6		5.44	2.14	38.2
NP HCl 0.5%	0.6	1.46	1.90	0.44	19.4
NP HCl 0.1%	0.6	1.89	5.28	3.39	51.6
	1.2		5.72	3.83	19.6

Special attention must be given to the yielding, accounting for the total mass recovered. In general, it is not possible to yield 100% of NP just by considering the total amount of chitosan and TPP masses put in the system. Moreover, some contaminants like salt as  $\text{CH}_3\text{COO}^-\text{Na}^+$  may be present in the NP, and there is no clear trend relating NP yielding production and pH solution.



**4.1 INFLUENCE OF THE ACID IN THE NP SIZE AND ZETA POTENTIAL**

The NP properties showed to have a high dependence on the type and concentration of acids (Table 2). For the first three entries, with fixed chitosan ( $3.0 \text{ mg cm}^{-3}$ ) and TPP ( $1.2 \text{ mg cm}^{-3}$ ) concentrations, the decreasing of acetic acid concentration resulted in a concomitant increase of the NP size. For NP HAc 0.1% and TPP  $1.2 \text{ mg cm}^{-3}$ , the suspension precipitated spontaneously. This result confirms that the acid concentration plays an important role in the NP formation. Also, the pH variation before and after reaction synthesis gives more information about the NP structure (Table 1).

Specifically for HAc 0.1%-TPP  $1.2 \text{ mg cm}^{-3}$ , it has a high pH variation (Table 1), indicating that the formation of NP is highly pH equilibrium dependent. A similar effect can be found in other reported studies. For example, using NaOH for pH adjustment in the chitosan solution leads to an increase in the NP size [1]. On the other hand, a reduction in the pH of the TPP solution with acid addition before the NP synthesis generates NP with smaller sizes [20]. Probably, the reactivity of the undissociated formed species (Eq. 1) represents the real force that drives the NP formation. The low value found for the zeta potential for the system NP HAc 0.1% and TPP =  $1.2 \text{ mg cm}^{-3}$  (Table 2) is compatible with its low stability. The weak net of positive charges established around the particles resulted in their instability and precipitation.

**Table 2.** Size, polydispersity index and zeta potential variations in the synthesis of NP from chitosan solution ( $3.0 \text{ mg cm}^{-3}$ ) in HCl and acetic acids solutions at different concentrations.

<b>Samples</b>	<b>TPP conc. (<math>\text{mg cm}^{-3}</math>)</b>	<b>Size (nm)</b>	<b>PdI</b>	<b>Zeta Potential (mV)</b>
NP HAc 1.0%	1.2	$135 \pm 7$	$0.42 \pm 0.02$	$29 \pm 1$
NP HAc 0.5%	1.2	$142.4 \pm 0.3$	$0.300 \pm 0.009$	$25 \pm 2$
NP HAc 0.1%	1.2	$1011 \pm 42$	$0.51 \pm 0.04$	$10.8 \pm 0.4$
	0.6	$653 \pm 14$	$0.56 \pm 0.02$	$38 \pm 1$
NP HCl 0.5%	0.6	$287 \pm 19$	$0.6 \pm 0.1$	$36 \pm 2$
	0.6	$538 \pm 13$	$0.54 \pm 0.05$	$48 \pm 1$
NP HCl 0.1%	0.6	$538 \pm 13$	$0.54 \pm 0.05$	$48 \pm 1$
	1.2	$615 \pm 18$	$0.27 \pm 0.02$	$19.9 \pm 0.5$

Therefore, the synthesis of NP exclusively from protonated chitosan and TPP, without any excess of  $\text{H}^+$ , is not a trivial task due to the TPP equilibrium. However, by decreasing the TPP concentration to  $0.6 \text{ mg cm}^{-3}$  and keeping the HAc at the low level (0.1%), the system was shifted

to a better condition (low NP size e high zeta potential). Although, the NP size range was higher than that found for NP HAc 1.0%.

For NP generated from the HCl solution, the results were very similar (Table 2). At fixed chitosan ( $3.0 \text{ mg cm}^{-3}$ ) and TPP ( $0.6 \text{ mg cm}^{-3}$ ) concentrations, the decreasing in the HCl concentration from 0.5% to 0.1% resulted in NP size increasing. Additionally, by reducing HCl to 0.1% and TPP increased to  $1.2 \text{ mg cm}^{-3}$ , the system became unstable, resulting in large NP sizes and low zeta potential values.

Comparing HAc and HCl as solvents, HCl reveals as a possible alternative for chitosan NP production, since, in general, by using this acid the resultant NP have higher zeta potential than those found when using HAc, what is a consequence of a more stable reducing agglomeration. Further, the NP size is smaller than those measured for the HAc system, mainly when using HCl at 0.1%.

The polydispersity index variation did not exhibit any trend with the type of acid anion nor its concentration, presenting an intermediary polydispersity index.

#### 4.2 MORPHOLOGICAL ASPECTS

Besides the size, the morphological characteristics of the chitosan NP play an important role in its functionality, especially concerning the delivery of active compounds and the antibacterial activity [21,22]. The most effective particle shape for bacterial interaction is spherical and small in size, in order to penetrate through the bacterial membrane and target the internal components of the cell [20].

However, the isolation of NP to achieve nanopowder is a challenging task due to the polyelectrolyte nature of the components, resulting in dense agglomerates. Depending on the intensity of such cohesive forces, the nanopowder is not able to be re-suspended in an aqueous medium after the lyophilization. Observations carried out by SEM analysis showed that NP obtained at the high acid concentration (HAc 1.0%) after lyophilization, showed an intense agglomeration with flake-like structure (Figure 2a), not allowing individual NP identification (Figure 2d). However, when acid concentration was decreased (HAc 0.5% and HAc 0.1%) a flake-like structure remained at low magnification (Figures 2b,c), but at high magnification, the NP structure was evidenced (Figure 2e,f). This is a significant result, which shows that the reactional condition has a strong influence on the isolation process of the material. Based on this, it is possible to conclude some role of the acid concentration. The highest acid concentration resulted in NP with low size (Table 2 - HAc 1.0% - 1.2 TPP), but such excess of acid in the reactional medium did not allow the isolation of a nanopowder with NP characteristics. On the other hand, regarding the

lowest acid concentration, NP was a little great in size (Table 2 - HAc 0.1% - 1.2 TPP), but some of its characteristics were preserved.

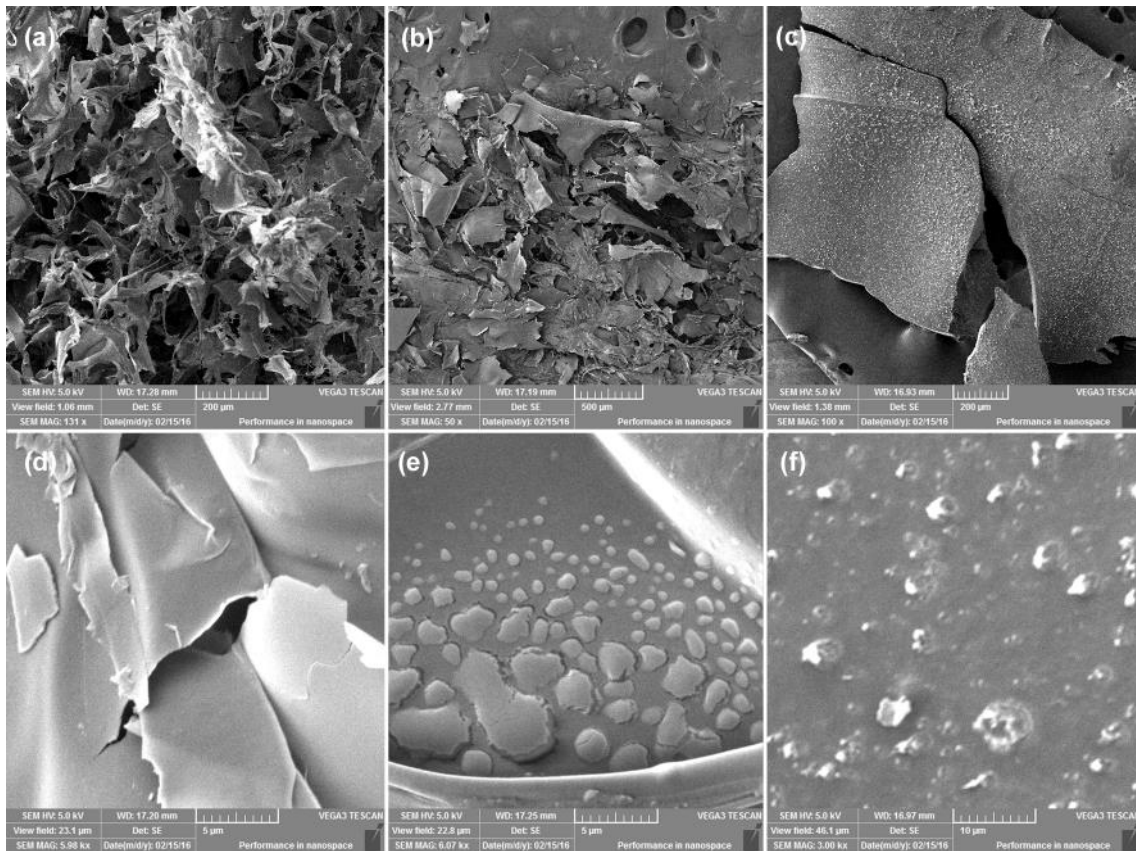


**Figure 2.** SEM images for freeze-dried samples of NP HAc 1.0% - 1.2 TPP (a, c); NP HAc 0.5% - 1.2 TPP (b, d) and NP HAc 0.1% - 1.2 TPP (c, f) with low (a, b and c) and high (d, e and f) magnifications.

To better understanding the isolation process, before lyophilization the NP suspension was preserved by cryoprotection (aqueous solution of sucrose). In this way, it is possible to obtain a powder finely divided with good form-suspension ability after sucrose washing out. The OM was a helpful technique for pre-evaluation of the suspensions. For sample with high TPP concentration (NP HCl 0.1% - 1.2 TPP), that resulted in large-sized NP (Table 2), the agglomeration was so intense that even after the treatment by cryoprotection, the NP did not re-suspended anymore, remained precipitated [23]. On the other hand, for HAc at the same condition (NP HAc 0.1% - 1.2 TPP), after freeze-drying with cryoprotection, the sample exhibit a good re-suspended aspect (Figure 3). Based on this, it is possible to affirm that in the presence of a high amount of TPP, the interparticle interaction (driven force for agglomeration) is strongest in HCl than in HAc.

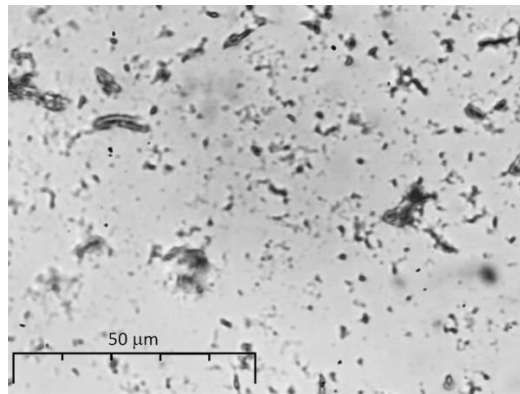


**Figure 3.** OM image for sample NP HAc 0.1% - 1.2 TPP after the treatments cryoprotection, lyophilization and re-suspend in water.

This previous analysis enables us to select only special samples for MEV analysis (Figure 4). By comparing such pictures with those took previously (Figure 2), it is clear that the cryogenic process preserves the NP structure. From MEV pictures, it seems that the sample NP HCl 0.1% - 0.6 TPP had a well-defined spherical shape but lost its spherical shape and trend to agglomerate when TPP was increased in the sample NP HCl 0.1% - 1.2 TPP (Figures 4a,b). This is an agreement with discussed above that, at fixed acid concentration, the increase in the TPP concentrations resulted in less effective NP formation. A similar result was found for NP HAc 0.1% - 0.6 TPP and NP HAc 0.1% - 1.2 TPP, in which the agglomeration was more intense for high TPP concentrations (Figures 4c,d). It has become evident that the pH is fundamental in stabilizing the NP structure once samples obtained with low acid concentration and high TPP concentration showed great pH variation, large size, high instability by zeta potential and morphological irregularities. Several drying techniques, e.g., freeze, spray and spouted bed drying, have been proposed in the literature to produce high-quality solid products [24]. However, the freeze-drying with cryoprotection looks to maintain better NP characteristics [25].



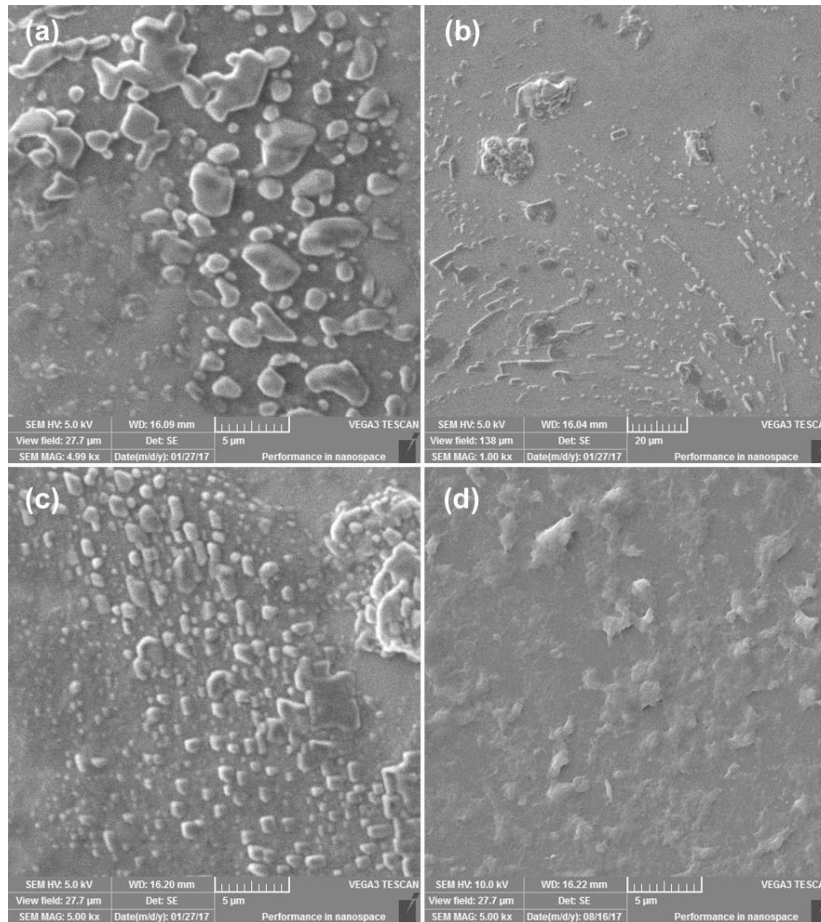


**Figure 4.** SEM images for freeze-dried samples previously preserved via cryoprotection treatment with sucrose at 5% (w/v) for a) NP HCl 0.1% - 0.6 TPP b); NP HCl 0.1% - 1.2 TPP; c) NP HAc 0.1% - 0.6 TPP and d) NP HAc 0.1% - 1.2 TPP.

#### 4.3 PROPERTIES OF ENCAPSULATED OF POLYPHENOLS

The encapsulation process implies a deep change in the NP structure [26]. First, it is observed an increase in the NP size. By DLS measurement, the average size was 700 nm. According, by SEM analysis, it is found NP size near such values (Figure 5). However, despite the efficiency of the cryoprotection in to isolate the NP, some NP agglomerate still present. The increase in the NP size was discussed before and can be attributed to the intensity of the interaction between the substance and TPP and between the substance and chitosan [5]. Generally, for each kind of encapsulated material, a new amount of TPP must be empirically established. Specifically for skin grape extract, the encapsulation efficiency was near 70%. This value is also dependent on the solubility of the substance [26].

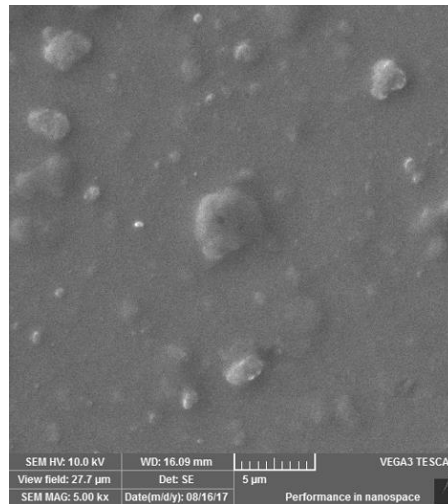


**Figure 5.** SEM image for freeze-dried NP HAc 0.5% sample encapsulated with skin grape extract and previously preserved via cryoprotection treatment with sucrose at 5% (w/v).

The release profile in normalized parameters is very similar for all the studied systems (Figure 6). The profiles exhibit an initial burst release, reaching a plateau after 5 hours of liberation [5]. In this way, independently of the solvent used to solubilize the chitosan and, also the physical state of the isolated NP if a wet or dry sample, the release profile followed a similar behavior.

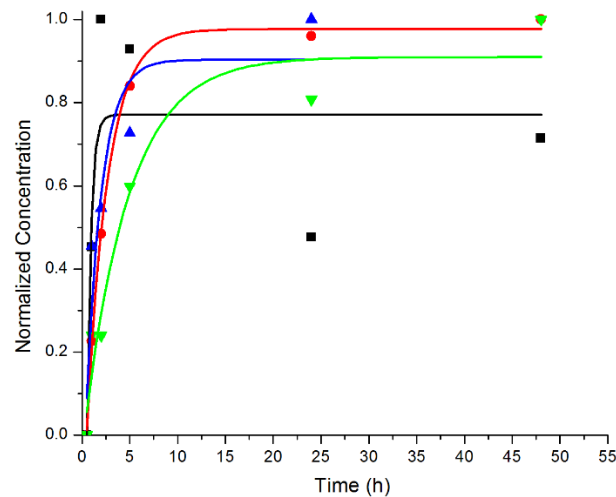


**Figure 6.** Release profiles for NP encapsulated with skin grape extract for NP HAc 5% wet (■); NP HAc 5% dry (●); NP HCl 5% wet (▲) and NP HCl 5% dry (▼) samples in the binary solution 0.6 ethanol : 0.4 phosphate buffer (pH = 7.4). The data were fit by an exponential decay ( $y = A1 \cdot \exp(-x/t1) + y0$ ), resulting the respective  $R^2$ : 0.54642; 0.99717; 0.79274 and 0.92584.

On the other hand, the release profile was deeply influenced by the pH medium. The grape extract release was greatly more favorable in acid, intermediate in neutral and very little in alkaline media (Figure 7). This may be related with to two phenomena a) better solubility of the grape extract in acid medium or b) change of conformation of NP structure in acid medium, leaving grape



extract less strongly bound to NP structure. Such a result confirms that the solvent physical-chemistry property plays a fundamental role in the release profile [5].

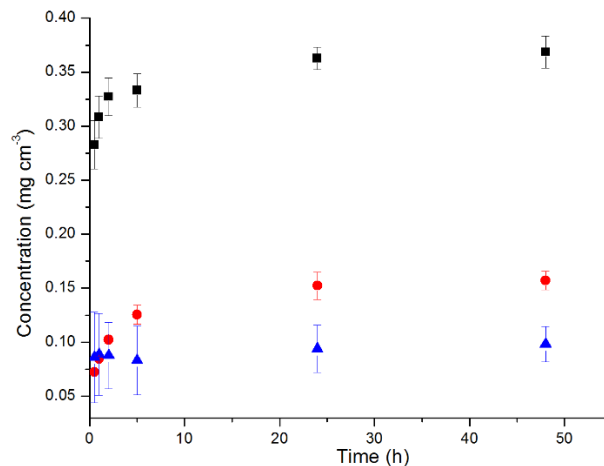


**Figure 7.** Release profiles for NP HAc 5% wet encapsulated with skin grape extract in the binary solution 0.6 ethanol : 0.4 phosphate buffer with different pH as: pH = 3.0 (■); pH = 7.0 (●) and pH = 10.0 (▲).

## 5 CONCLUSION

The most relevant factor that affected the chitosan-TPP NP structure was the low concentration of acid solution allied with a high concentration of TPP, resulting in high pH variation before and after the synthesis, bad re-suspension in water after freeze-dried and formation of morphological defects like large agglomeration. HCl can be used indistinctly to synthesize NP from chitosan and TPP. The strategy of pre-treatment with cryoprotection solution of sucrose was adequate to preserve the NP structure and potentially useful for isolation in large scale, for example. All the systems are suitable for encapsulation and release application of skin grape extract. However, the substance release is highly favorable in acid medium.

## ACKNOWLEDGEMENT

This study was supported by Fundação de Amparo à Ciência e Tecnologia do Estado de Pernambuco, FACEPE (grantnumbers APQ-0757-1.06/14 and BFT 0019-1.06/15). The authors are thankful to RedeAgroNano (Embrapa) and CNPq for financial support. Also, special thanks to Adriana CoatriniThomazi (Embrapa Instrumentation) and Ginetton Ferreira Tavares (Science Material Lab. - UNIVASF) to collect the DLS and SEM data, respectively.

**REFERENCES**

- [1] Gan Q., Wang T., Cochrane C., McCarron P. Modulation of surface charge, particle size and morphological properties of chitosan–TPP nanoparticles intended for gene delivery. **Colloids and Surfaces B: Biointerfaces**v. 44, p.65-73, 2005.
- [2] Bulmer C., Margaritis A., Xenocostas A. Production and characterization of novel chitosan nanoparticles for controlled release of rHu-Erythropoietin. **Biochemical Engineering Journal**v. 68, p. 61-69, 2012.
- [3] Kiilll C.P., Barud H.S., Santagneli S.H., Ribeiro S.J.L., Silva A.M., Tercjak A., Gutierrez J., Pironi A.M., Gremião M.P.D. Synthesis and factorial design applied to a novel chitosan/sodium polyphosphate nanoparticles via ionotropic gelation as an RGD delivery system. **Carbohydrate Polymers**v. 157, p. 1695-1702, 2017.
- [4] Lamarra J., Rivero S., Pinotti A. Design of chitosan-based nanoparticles functionalized with gallic acid. **Materials Science and Engineering Cv**. 67, p. 717-726, 2016.
- [5] Britto D., Moura M.R., Aouada F.A., Pinola F.G., Lundstedt L.M., Assis O.B.G., Mattoso L.H.C. Entrapment characteristics of hydrosoluble vitamins loaded into chitosan and N,N,N-trimethyl chitosan nanoparticles. **Macromolecular Research**v. 22, p. 1261-1267, 2014.
- [6] Hussein-Al-Ali S.H., Kura A., Hussein M.Z., Fakurazi S. Preparation of chitosan nanoparticles as a drug delivery system for perindopril erbumine. **Polymer Composites**v. 39, p. 544-552, 2018. <https://doi.org/10.1002/pc.23967>
- [7] Yu X., Jing Y., Jiang Y. Preparation of proanthocyanidin–chitosan complex and its antioxidant and antibacterial properties. **Iranian Polymer Journal**v. 27, p. 653, 2018. <https://doi.org/10.1007/s13726-018-0642-5>
- [8] Najafabadi A.H., Abdouss M., Faghihi S. Synthesis and evaluation of PEG-O-chitosan nanoparticles for delivery of poorly water-soluble drugs: Ibuprofen. **Materials Science and Engineering Cv**. 41, p. 91-99, 2014.
- [9] Munteanu B.S., Sacarescu L., Vasiliu A.L., Hitruc G.E., Pricope G.M., Sivertsvik M., Rosnes J.T., Vasile C. Antioxidant/antibacterial electrospun nanocoatings applied onto PLA films. **Materials**v. 11(10), 1973, 2018. <https://doi.org/10.3390/ma11101973>

- [10] Glaser T.K., Plohl O., Vesel A., Ajdnik U., Ulrih N.P., Hrnčič M.K., Bren U., Zemljic L.F. Functionalization of polyethylene (PE) and polypropylene (PP) material using chitosan nanoparticles with incorporated resveratrol as potential active packaging. **Materials**v. 12(13), p. 2118, 2019. <https://doi.org/10.3390/ma12132118>
- [11] Yang H., Tian T.T., Wu D.H., Guo D.J., Lu J. Prevention and treatment effects of edible berries for three deadly diseases: Cardiovascular disease, cancer and diabetes. **Critical Review in Food Science**v. 59(12), p. 1903-1912, 2019.
- [12] Zhang L., Kosaraju S.L. Biopolymeric delivery system for controlled release of polyphenolic antioxidants. **European Polymer Journal**v. 43, p. 2956-2966, 2007. <https://doi.org/10.1016/j.eurpolymj.2007.04.033>
- [13] Nguyen V.C., Nguyen V.B., Hsieh M.-F. Curcumin-Loaded Chitosan/Gelatin Composite Sponge for Wound Healing Application. **International Journal Polymer Science** Article ID 106570, 7 pages, 2013. <https://doi.org/10.1155/2013/106570>
- [14] Cerruti P., Santagata G., d'Ayala G.G., Ambrogi V., Carfagna C., Malinconico M., Persico P. Effect of a natural polyphenolic extract on the properties of a biodegradable starch-based polymer. **Polymer Degradation and Stability**v. 96, p. 839-846, 2011. <https://doi.org/10.1016/j.polymdegradstab.2011.02.003>
- [15] Bonilla J., Sobral P.J.A. Antioxidant and physicochemical properties of blended films based on gelatin-sodium caseinate activated with natural extracts. **Journal of Applied Polymer Science**v. 134, 44467, 2017. <https://doi.org/10.1002/APP.44467>
- [16] Desai K.G.H. Chitosan nanoparticles prepared by ionotropic gelation: An overview of recent advances. **Critical Reviews in Therapeutic Drug Carrier Systems**v. 33, p. 107-158, 2016.
- [17] Moura R.S., Pires K.M.P., Ferreira T.S., Lopes A.A., Nesi R.T., Resende A.C., Sousa P.J.C., Silva A.J.R., Porto L.C., Valença S.S. Addition of açai (*Euterpe oleracea*) to cigarettes has a protective effect against emphysema in mice. **Food and Chemical Toxicology**v. 49(4), p. 855-863, 2011.
- [18] Argüelles-Monal W., Cabrera G., Peniche C., Rinaudo M. Conductimetric study of the interpolyelectrolyte reaction between chitosan and polygalacturonic acid. **Polymer**v. 41, p. 2373-2378, 2000.

- [19] Corbridge, D.E.C. **Phosphorus: Chemistry, Biochemistry and Technology**. 6th Edition. CRC Press, Boca Raton, 2013. Chap. 5, pg. 185.
- [20] Masarudin M.J., Cutts S.M., Evison B.J., Phillips D.R., Pigram P.J. Factors determining the stability, size distribution, and cellular accumulation of small, monodisperse chitosan nanoparticles as candidate vectors for anticancer drug delivery: application to the passive encapsulation of [14C]-doxorubicin. **Nanotechnology, Science and Applications** v. 8, p. 67-80, 2015.
- [21] Cota-Arriola O., Cortez-Rocha M.O., Ezquerro-Brauer J.M., Lizardi-Mendoza J., Burgos-Hernandez A., Robles-Sanchez R.M., Plascencia-Jatomea M. Ultrastructural, morphological, and antifungal properties of micro and nanoparticles of chitosan crosslinked with sodium tripolyphosphate. **Journal of Polymers and the Environmental** v. 21, p. 971-980, 2013.
- [22] Leonida M.D., Banjade S., Vo T., Anderle G., Haas G.H., Philips N. Nanocomposite materials with antimicrobial activity based on chitosan. **International Journal of Nano and Biomaterials** v. 3, p. 316-334, 2011.
- [23] Tang K.S., Hashmi S.M., Shapiro E.M. The effect of cryoprotection on the use of PLGA encapsulated iron oxide nanoparticles for magnetic cell labelling. **Nanotechnology** v. 24, 125101 (8pp), 2013.
- [24] Gallo L., Piña J., Bucalá V., Allemandi D., Ramírez-Rigo M.V. Development of a modified-release hydrophilic matrix system of a plant extract based on co-spray-dried powders. **Powder Technology** v. 241, p 252-262, 2013.
- [25] Shahgaldian P., Gualbert J., Aissa K., Coleman A.W. A study of the freeze-drying conditions of calixarene based solid lipid nanoparticles. **European Journal of Pharmaceutics and Biopharmaceutics** v. 55, p. 181-184, 2003.
- [26] Yew H.C., Misran M. Preparation and characterization of pH-dependent  $\kappa$ -carrageenan-chitosan nanoparticle as potential slow release delivery carrier. **Iranian Polymer Journal** v. 25, 1037, 2016. <https://doi.org/10.1007/s13726-016-0489-6>